COBEM 2023 27TH INTERNATIONAL CONGRESS OF MECHANICAL ENGENEERING

ABCM Brazilian Society of Mechanical Sciences and Engineering
27th ABCM International Congress of Mechanical Engineering
December 04-08, 2023, Florianópolis-SC, Brazil

COB-2023-0242
THERMOMECHANICAL CHARACTERIZATION OF A CU-AL-MN SHAPE MEMORY ALLOY OBTAINED BY INVESTMENT CASTING

Railson de Medeiros Nóbrega Alves
Postgraduate Program in Mechanical Engineering, Federal University of Paraíba, João Pessoa – PB, Brazil
railson.nobrega@gmail.com

Paulo César Sales da Silva
Postgraduate Program in Process Engineering, Federal University of Campina Grande, Campina Grande – PB, Brazil
paulocesarsales@outlook.com

Rodinei Medeiros Gomes *(in memoriam)*
Department of Mechanical Engineering, Federal University of Paraíba, João Pessoa – PB, Brazil
rodineix@gmail.com

Danielle Guedes de Lima Cavalcante
Department of Mechanical Engineering, Federal University of Paraíba, João Pessoa – PB, Brazil
danielleguedes02@gmail.com

Carlos José de Araújo
Department of Mechanical Engineering, Federal University of Campina Grande, Campina Grande – PB, Brazil
carlos.jose@professor.ufcg.edu.br

Abstract. *Shape Memory Alloys (SMA) are unique metallic alloys capable of recovering their shape when subjected to significant deformations and appropriate thermal cycles, even under loading. These alloys exhibit two distinctive functional properties: Superelasticity (SE), allowing for the recovery of large deformations and mechanical hysteresis, and the shape memory effect (SME), enabling the recovery of apparent plastic deformations through heating. Cu-Al-based SMAs, incorporating elements like Mn, Ni, and Be, offer cost-effective alternatives to NiTi alloys and find applications due to their wide range of transformation temperatures and compatibility with conventional metallurgical processes. The aim of this study was to characterize the thermomechanical behavior of a 83Cu-12Al-5Mn (wt%) SMA. The SMA was produced through arc melting and injected into ceramic molds via centrifugation. Differential Scanning Calorimetry (DSC) was used to determine the phase transformation temperatures, indicating the presence of a martensitic structure at room temperature. Quasi-static tensile tests as a function of temperature were conducted to investigate mechanical properties and observe the transition from SME to SE behavior. Dynamic Mechanical Analysis (DMA) was employed to assess the material's elasticity modulus and damping capacity across different temperatures. Furthermore, the SMA demonstrated proper thermomechanical behavior and superior damping capacity compared to conventional metallic alloys, highlighting its potential for mechanical component production.*

Keywords: *Shape memory alloys; Cu-Al-Mn alloys; Thermomechanical properties; Shape memory effect; Investment casting.*

1. INTRODUCTION

Shape Memory Alloys (SMAs) are smart metallic materials that possess the ability to respond to thermomechanical stimuli through the phenomena of Shape Memory Effect (SME) and Superelasticity (SE). These effects enable the recovery of significant levels of seemingly plastic deformations, achieved through heating and mechanical loading, respectively (Huang et al., 2010; Lagoudas, 2008).

Due to these remarkable functional properties, SMAs have found applications in various advanced engineering fields, including biomedical, automotive, aerospace, and oil and gas industries, among others (Otsuka & Wayman, 1998). The most commonly utilized SMAs are nickel-titanium (NiTi) based alloys (such as NiTi, NiTiCu, NiTiNb) and copper-based alloys derived from the Cu-Al and Cu-Zn binary systems.

Despite the widespread commercial use and excellent biocompatibility of NiTi SMAs, their processing challenges and high cost have necessitated the exploration of alternative materials and alloys.

Therefore, copper-aluminum-based SMAs (CuAl) have emerged as a subject of extensive research related to SME and SE phenomena. Compared to NiTi SMAs, CuAl based alloys offer advantages such as higher phase transformation temperatures, significantly lower cost, and the ability to achieve desired properties through the addition of ternary

chemical elements (e.g., Mn, Ni, Be, Nb,….) (Sutou et al., 1999; Kumar et al., 2015). However, challenges associated with this alloy system include controlling the transformation temperatures through the addition of a third element and addressing the brittleness of polycrystalline alloys when operated at low temperatures.

In this context, the present study aimed to fabricate and thermomechanically characterize a CuAl-based SMA. A specific composition within the CuAlMn system was determined, allowing the alloy to exhibit a martensitic structure at room temperature for the SME phenomenon and demonstrate SE upon heating. For the manufacturing of the CuAlMn SMA, the pure metals were molten by plasma arc melting in a process called plasma skull push–pull (PSPP) (De Araújo et al., 2009), followed by investment casting and injection into ceramic molds using centrifugation. Test specimens were obtained to characterize the SMA through thermal analysis using DSC, tensile testing at different temperatures, DMA in a single cantilever beam mode and optical microscopy analysis testing.

2. MATERIALS AND METHODS

The activities undertaken in this study were conducted at the Multidisciplinary Laboratory of Active Materials and Structures (LaMMEA), which is affiliated with the Academic Unit of Mechanical Engineering (UAEM) at UFCG. The experimental procedure employed in this study is presented through the block diagram depicted in the Figure 1.

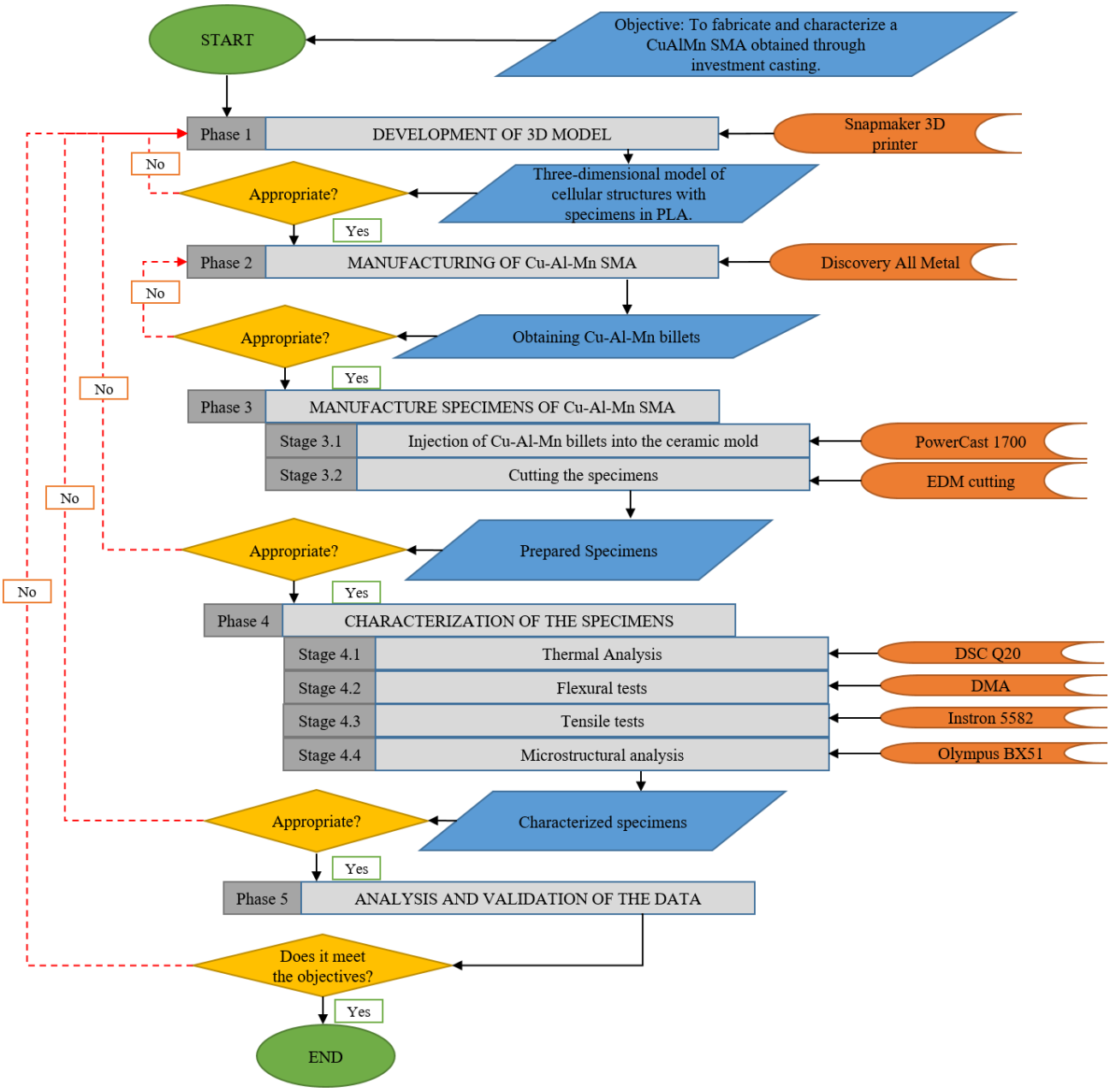

Figure 1. Methodological process used in the development of the research.

2.1 Manufacture of SMA CuAlMn specimens

Initially, it were designed dog bone and plate-type specimens CAD models. Subsequently, 3D models were printed using PLA material on a Snapmaker 3D Printer. The CuAlMn test specimen's were obtained through the electrical discharge machining (EDM) process.

To obtain the solid molds from the tree containing the PLA model, the Calibra Express ceramic coating (an ultra-thin coating for casting metallic alloys) was employed. Once the mold is prepared, it undergoes ambient temperature drying for 60 minutes to solidify the coating around the model. Subsequently, this assembly is placed in an electric furnace for curing, following the instructions provided by the coating supplier. After this step, the PLA is evaporated, resulting in a ceramic-coated mold of the desired component.

For this study, a CuAlMn SMA composition was selected based on the study of Santana et al. (2018). The composition corresponds to approximately 83Cu-12Al-5Mn (wt%), using commercially pure elements (purity exceeding 99%). Small buttons (approximately 15 grams) of this alloy were produced using the PSPP process on the Discovery All Metal machine. To ensure a good homogeneity, the obtained CuAlMn SMA buttons were re-melted four times. The SMA buttons were then melted one last time before being injected into the test specimen's ceramic mould using an induction melting with centrifugal casting (ICC) process, using the PowerCAST 1700 machine. The temperature of the ceramic mold at the time of injection was approximately 250 °C. In this process, once the metal is molten, centrifugal injection is carried out into the mold, shaping the desired piece. After injection, the mold undergoes rapid cooling in water at room temperature. This cooling process corresponds to quenching and aims to induce the phase transformation characteristic of CuAl SMAs. The entire process is completed in approximately 3 minutes. More details concerning this process can be obtained in the recent work of Albuquerque, Grassi & De Araújo (2023).

After completion of the casting process and with the cooled mold, the test specimens were demolded. After cleaning via alumina powder blasting, the samples were subjected to wire EDM cutting, after that the specified dimensions in Figure 2 were obtained. Following the cutting of the samples, a grinding step was performed using a 1200 µm grid sandpaper to prepare the material for characterization.

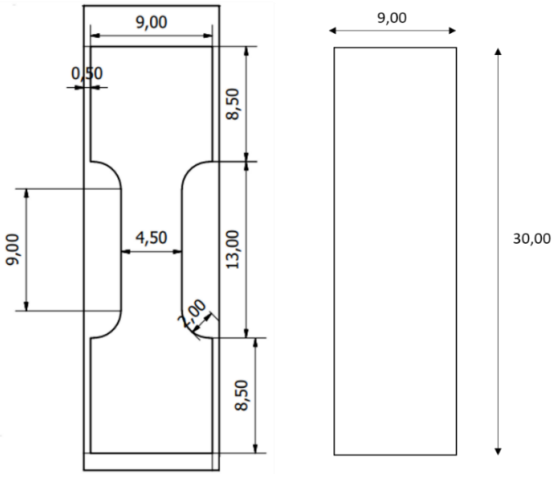

Figure 2. Illustration of the test specimen's (dog-bone and plate) with their respective dimensions in mm.

2.2 Characterization of the CuAlMn SMA specimens

The characterization of the CuAlMn SMA specimens was conducted in the following sequence:

1. The thermal behavior was analyzed by Differential Scanning Calorimetry (DSC) technique, using a Q20 calorimeter from TA Instruments, following the ASTM F2004-05 standard and applying a heating and cooling rate of 10°C/min. The identification of the transformation temperatures of the samples were obtained by the tangent intersection method of the DSC peaks.
2. Thermomechanical tensile tests were carried out to analyze the performance of the dogbone sample (Fig. 2) at different temperatures (30°C, 50°C, 70°C, 90°C, 110°C, 130°C, and 150°C) and with mechanical loadings up to 7% deformation, allowing the observation of the SME and SE behaviors. A thermal chamber was employed, and a 30-minute waiting period was observed to ensure the stabilization of the programmed temperature. These tests followed the ASTM-2516/07 standard, which recommends a deformation rate of 1% min^{-1}. After each isothermal test, the sample underwent a simple heating process ($T>A_f$) to minimize residual deformations.

3. Dynamic Mechanical Analysis (DMA) tests were performed in simple bending and single cantilever modes to evaluate the material's behavior under dynamic loading. The damping capacity, represented by the tangent of the phase angle (*Tan δ*), and the modulus of elasticity, represented by the elastic component and associated with the material's stiffness, were determined. The specimens were subjected to a displacement of 10μm, with a frequency of 1.0 Hz, and the temperature ranged from 30°C to 150°C at a rate of 2°C/min^{-1}.

4. Microstructural analysis (Olympus, BX51 model) was carried out to identify the distribution of grains in the produced alloy. For this characterization, the samples were prepared using standard metallographic techniques: grinding with sand paper (up to 1200 mesh), followed by polishing in alumina solution with granulometry of 1.0, 0.3 and 0.05 μm.

3. RESULTS AND DISCUSSIONS

3.1 Thermal Analysis

Figure 3 illustrates the phase transformation temperatures of SMA CuAlMn specimens.

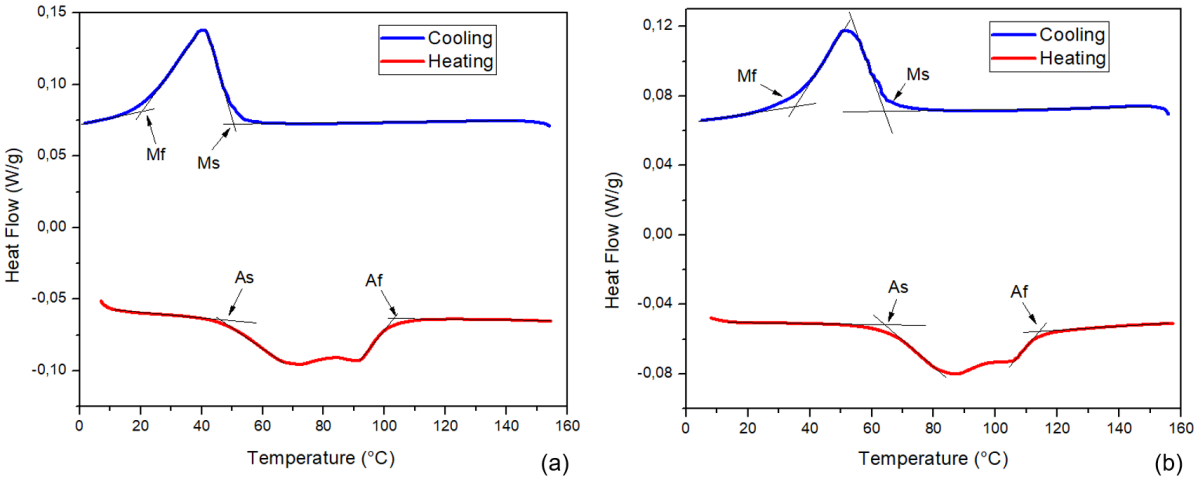

Figure 3. DSC thermal behavior of as-cast CuAlMn SMA samples (a) plate-type and (b) dog-bone.

Analysis of Figure 3 demonstrates that SMA CuAlMn undergoes phase transformation even in its as-cast state. Table 1 provides the transformation temperatures of the obtained specimens from Fig. 3. It is evident that both specimens exhibited a potential for SME when subjected to deformations at room temperature (approximately 25°C) and heated to about 120ºC. The transformation temperatures of dog-bone and plate specimens exhibited close proximity, indicating effective control over the chemical composition during the casting process.

Table 1. Phase transformation temperatures for CuAlMn SMA.

DSC	M_s (ºC)	M_f (ºC)	A_s (ºC)	A_f (ºC)
Dog-bone	32.5	64.1	64.2	114.1
Plate-type	20.5	50.6	46.1	103.0

3.2 Tensile mechanical tests for the dogbone specimens

The dog-bone specimen was subjected to uniaxial tensile testing at isothermal conditions ranging from 30°C to 150°C, as shown by the results in Figure 4. The response of the material can be observed at temperatures where it is fully martensitic and austenitic. The red curves represent temperatures near or above A_f, indicating superelastic behavior.

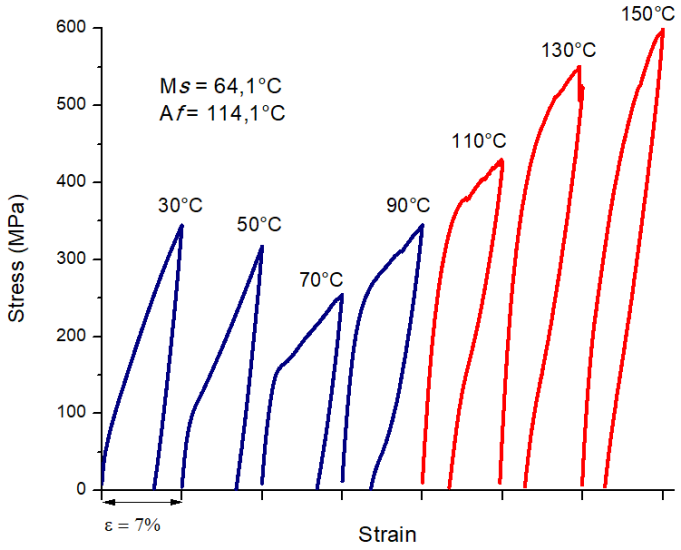

Figure 4. Mechanical response under uniaxial tension of CuAlMn SMA at different temperatures.

It is evident that with the onset of the formation of the ordered austenitic structure above 70°C (a temperature higher than A_s), there was a nearly linear increase in the maximum stress to complete the 7% cycle. It is also observed that the residual deformation decreased starting from 90 °C. This temperature is higher than the A_s temperature, indicating the onset of the SE phenomenon and explaining the decrease in residual deformation. In Figure 5, the behavior of residual deformation after the isothermal tests can be observed. It can be noted that the closer the temperature is to A_f, the smaller the residual deformation.

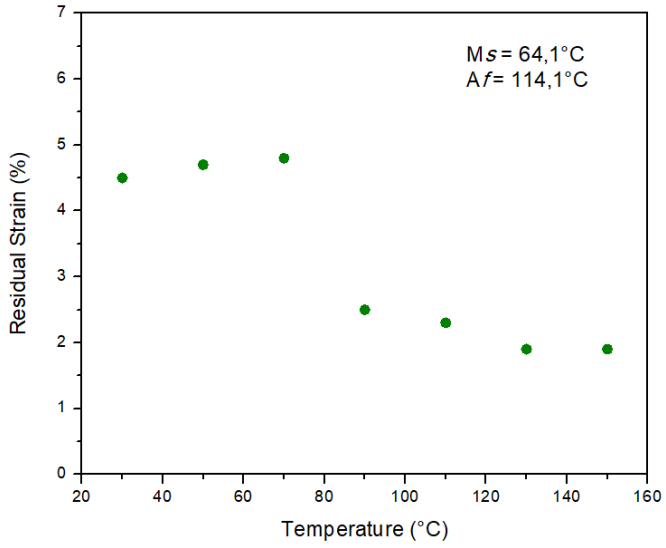

Figure 5. Levels of residual deformation at the end of each cycle in dog-bone specimens.

It is evident that when the specimen was subjected to temperatures within the martensitic phase range (30°C, 50°C, and 70°C), the residual deformations remained relatively constant, showing minimal variation within the range of 4.5% to 5%. As the temperature increased (90°C and 110°C), and particularly when the specimen exceeded the A_f temperature (130°C and 150°C), reaching a fully austenitic state, a significant drop of residual deformation was observed, ranging from 1.5% to 2.5%.

From Figure 4, it is also possible to extract the characteristic stresses for the initial martensite orientation (30°C, 50°C, and 70°C), as well as the stress-induced martensite from austenite (90°C, 110°C, 130°C, and 150°C). Between 70°C and 130°C the stress-strain relationship exhibited an approximately linear behavior with a Clausius-Clayperon slope, as depicted in Figure 6.

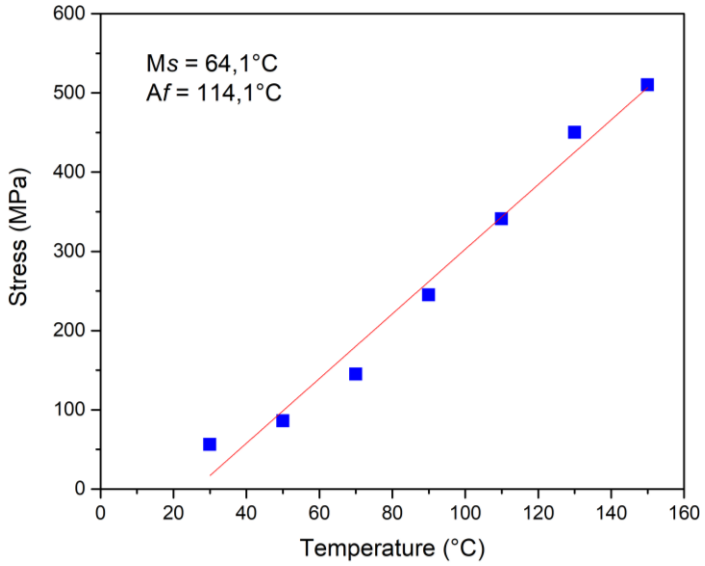

Figure 6. Characteristic stresses for initial orientation and martensite induction of the CuAlMn SMA as a function of temperature.

According to the classical Clausius-Clapeyron relationship, the transformation stresses of SMA can be approximated as a linear function of temperature. This relationship provides the correlation between force or stress and temperature along an equilibrium line for phase transformations (Otsuka & Wayman, 1998). In Figure 6, a linear relationship is observed within the temperature range of 70°C to 130°C, which is above M_s, indicating the presence of both phases.

According to Grassi et al. (2015), the Coefficient of Determination (R2) is a measure of how well the data is fitted to a statistical model, ranging from 0 to 1. The closer it is to 1 (100%), the better the generated model is adjusted. For this property, considering all the analyzed temperatures, a coefficient of determination of 97.58% was obtained, indicating a very good fit of the results to the model. However, when considering only the range between 70°C and 130°C, an even higher improvement in the coefficient of determination is observed, reaching a value of 99.90%. This demonstrates an exceptional fit of the results to the model in this specific temperature range.

A tensile test at a temperature of 30°C was performed to determine the maximum tensile strength of the specimens obtained through the ICC process. A new specimen (dog-bone) underwent an initial cycle in which it was loaded up to 6% deformation and then unloaded to 7 MPa. Following the unloading, the second cycle was initiated, and the specimen was loaded until fracture. Figure 7 depicts the behavior of the CuAlMn SMA during the aforementioned test.

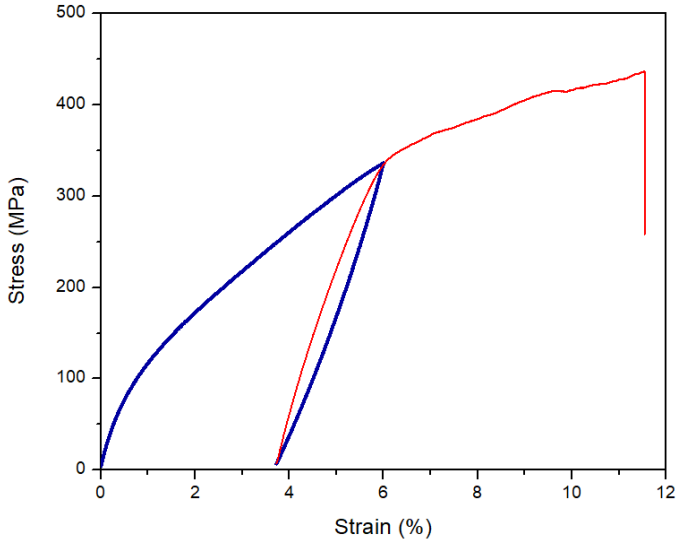

Figure 7. Stress-strain behavior for a CuAlMn SMA obtained by the ICC process.

It is observed that the test specimen, after unloading to 7 MPa, exhibited a residual deformation of approximately 3.7%. In the second cycle, it is observed that the CuAlMn test specimen withstands a deformation exceeding 11%. Simões

(2016) conducted the same test of a NiTi SMA with SME characteristics obtained through the same ICC process. The responses obtained for the CuAlMn SMA were similar to the one observed by Simões (2016) for a cast NiTi SMA, in terms of deformation.

3.3 Thermomechanical bending tests performed on the plate specimen using DMA

The behavior of the damping capacity (*Tan δ*) and the elastic modulus of the CuAlMn SMA can be observed in Figure 8.

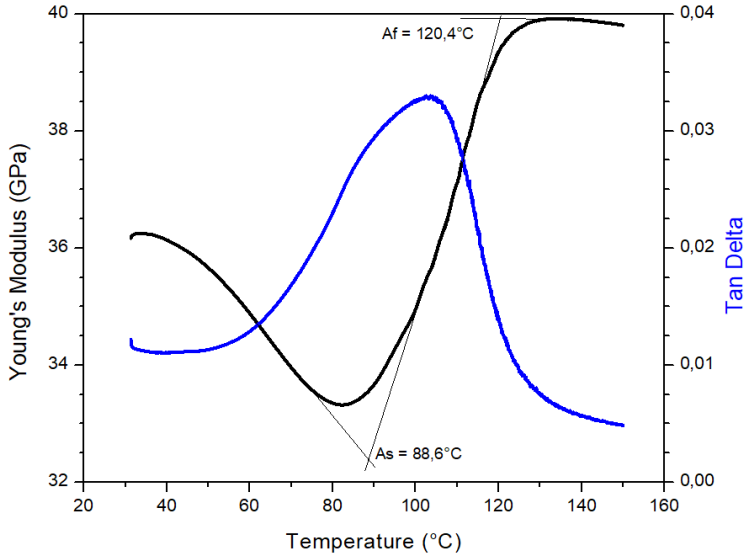

Figure 8. *Tan δ* and Young's modulus as a function of temperature for a CuAlMn SMA sample in DMA.

It can be observed in Figure 8 that the damping capacity of the CuAlMn SMA in the martensitic phase (approximately 30°C) exceeds 0.01 and is consequently higher than that of high damping metals (Hidamets). Hidamets, as reported by Vandeurzen et al. (1981), are metals that exhibit a high damping capacity, with values around 0.01 for *Tan δ*. This damping capacity further increases with heating, reaching a maximum value (~0.033) at a temperature close to 100°C. One characteristic of SMAs regarding damping capacity behavior is the presence of a damping peak during the phase transformation from the martensitic to the austenitic state. Subsequently, a decrease in damping capacity is observed. According to Silva et al. (2011), this reduction is attributed to the low absorption of mechanical energy by the austenite phase, in contrast to the martensitic structure composed of variants with higher mobility and energy dissipation. Silva et al. (2011) conducted a comparative study involving a NiTi SMA, aluminum, stainless steel, and brass, revealing that all conventional metals did not exhibit a damping capacity exceeding 0.01, with NiTi SMA demonstrating superiority.

Furthermore, Figure 8 provides insights into the behavior of the elastic modulus of the CuAlMn SMA at different temperatures. It can be observed that the elastic modulus increases as the temperature rises during the phase transformation (from a minimum value of 33.5 GPa to a maximum close to 40.0 GPa), which is a characteristic feature of SMAs. A similar behavior was observed by Silva et al. (2011) for a NiTi SMA.

3.4 Microstructural analysis of CuAlMn SMA

The plate-type specimen was analyzed using optical microscopy. The resulting microstructure is shown in Figure 9. It is evident that the grain morphology displays a martensitic phase with twinning at room temperature. This martensite structure can be identified by the needle-like structures formed within the grains. Moreover, the average grain size is approximately 130 μm, which is in accordance with the findings of Babacan et al. (2017), where diverse micrographs of a CuAlMn SMA subjected to various heat treatments are presented.

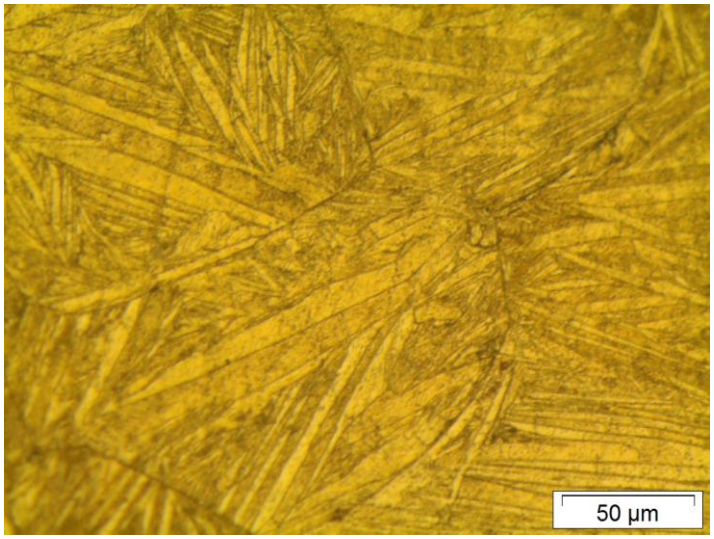

Figure 9. Optical image of the produced CuAlMn SMA.

4. CONCLUSIONS

The CuAlMn SMA exhibited phase transformation temperatures ranging from 20.5°C to 114.1°C. It is evident that as the temperature approaches the A_f temperature, the material undergoes the SE phenomenon. This is further supported by the observed decrease in residual deformations for temperatures close to A_f.

Based on the DMA test results conducted on plate-type specimens, it was determined that the CuAlMn SMA possesses excellent damping capacity ($Tan\delta$ higher than 0.01), surpassing that of conventional metallic alloys.

Through comprehensive analysis, it has been confirmed that the investment casting process employed in this study is a viable method for manufacturing both CuAlMn SMA and mechanical components using this material, which can be regarded as an advanced aluminum bronze.

ACKNOWLEDGENTS

The authors are grateful to Brazilian National Council for Scientific and Technological Development (CNPq) for the scholarship PQ-1C, grant number 302740/2018-0; the Paraiba State Research Support Foundation (FAPESQ-PB) for the project NISMArt, grant number 044/2023; and the CNPq for the doctoral scholarship to Railson de Medeiros Nóbrega Alves.

5. REFERENCES

Babacan, N.; Ma, J.; Turkbas, O. S.; Karaman, I. e Kockar, B.; The effects of cold rolling and the subsequent heat treatments on the shape memory and the superelasticity characteristics of Cu73Al16Mn11 shape memory alloy. Smart Materials and Structures. 2017.

da Silva Albuquerque, C.E., Grassi, E.N.D. & De Araújo, C.J. Castability of Cu-Al-Mn shape memory alloy in a rapid investment casting process: computational and experimental analysis. Int J Adv Manuf Technol 127, 2563–2579 (2023).

De Araújo, C. J.; Gomes, A. A. C.; Silva, J. A.; Cavalcanti, A. J. T.; Reis, R. P. B. e Gonzalez, C. H. Fabrication of shape memory alloy using the plasma skull push-pull process. Journal of materials processing technology, v. 209, n. 7, p. 3657-3664, 2009.

Grassi, E. N. D.; de Oliveira, H. M. R.; de Araujo, C. J.; de Castro, W. B. Effect of heat treatments on the thermomechanical behaviour of Ni-Ti superelastic mini coil springs. In MATEC Web of Conferences (Vol. 33, p. 03004). EDP Sciences. 2015.

Huang, W. M.; Ding, Z.; Wang, C. C.; Wei, J.; Zhao, Y. e Purnawali, H. Shape memory materials. Materials Today, v. 13, n. 7–8, p. 54–61, jul. 2010.

Kumar, P.; Jain, K. A.; Hussain, S.; Pandey, A. e Dasgupta, R., "Changes in the properties of Cu-Al-Mn shape memory alloy due to quaternary addition of different elements", Revista Matéria, Vol. 20, Rio de Janeiro, n. 1, pp. 284-292. 2015.

Lagoudas, D. Shape Memory Alloys: Modeling and Engineering Applications, Editora: Springer Science+Business Media, LLC, 2008.

Otsuka, K e Wayman, C.M. Shape Memory Materials, Cambridge University Press, Cambridge UK. p.1-131. 1998.

Santana, Y. N. de L.; Da Silva, P. C. S.; Calazans, R. N. D.; De Araújo, C. J. *Fabricação de Honeycombs de liga com Memória de Forma Cu-Al-Mn usando fundição de precisão. X Congresso Nacional de Engenharia Mecânica* (CONEM), Salvador, p. 1-7, 2018.

Silva, N. J.; De Araújo, C. J.; Gonzalez, C. H.; Grassi, E. N. D. e Oliveira, C. A. N., *Estudo comparativo das propriedades dinâmicas de uma liga NiTi com memória de forma e materiais estruturais clássicos. Revista Matéria*, v. 16, n. 4, pp. 830 – 835, 2011.

Simões, J. de B., *Fabricação de componentes miniaturizados de ligas com memória de forma Ni-Ti usando fundição de precisão.* 243 f., 2016. (Thesis) Postgraduate Program in Materials Science and Engineering, Federal University of Campina Grande, Campina Grande, 2016.

Sutou, Y.; Kainuma, R. e Ishida, K., "Effect of Alloying Elements on the Shape Memory Effect Properties of ductile Cu-Al-Mn Alloys." Materials Science and Engeneering, 1999.

Vandeurzen, U., Verelst, H. e Snoeys, R. “Dynamic properties of high damping metals”, Journal de Physique, v. 10, pp. 1169-1174, 1981.

6. RESPONSIBILITY NOTICE

The author(s) is (are) the only responsible for the printed material included in this paper.